

# TOWARD AN OPTIMIZED GLOBAL-IN-TIME SCHWARZ ALGORITHM FOR DIFFUSION EQUATIONS WITH DISCONTINUOUS AND SPATIALLY VARIABLE COEFFICIENTS

## PART 2 : THE VARIABLE COEFFICIENTS CASE

FLORIAN LEMARIÉ\*, LAURENT DEBREU†, AND ERIC BLAYO‡

**Abstract.** This paper is the second part of a study dealing with the application of a global-in-time Schwarz method to a one dimensional diffusion problem defined on two non-overlapping subdomains. In the first part, we considered that the diffusion coefficients were constant and possibly discontinuous. In the present study, we address the problem for spatially variable coefficients with a discontinuity at the interface between subdomains. For this particular case, we derive a new approach to determine analytically the convergence factor of the associated algorithm. The theoretical results are illustrated by numerical experiments with *Dirichlet-Neumann* and *Robin-Robin* interface conditions. In the *Robin-Robin* case, thanks to the convergence factor found at the analytical level, we can optimize the convergence speed of the Schwarz algorithm.

**Key words.** Optimized Schwarz Methods, Waveform Relaxation, Alternating and Parallel Schwarz Methods

**AMS subject classifications.** 65M55, 65F10, 65N22, 35K15, 76F40

### 1. Introduction.

**1.1. General context.** The overall context of the present work is the coupling between oceanic and atmospheric numerical models, in particular for representing processes in which the interactions between both media are of prime importance. The algorithms generally used to couple this type of numerical models are often not fully correct from a mathematical point of view. Indeed, they do not ensure a perfect consistency of the fluxes exchanged at the air-sea interface [8]. In this context, the long-term objective of our work is to derive alternative numerical techniques ensuring such a consistency, as well as to study their possible impact on the physical results of coupled models. Global-in-time *Optimized Schwarz Methods* (also called Schwarz waveform relaxation methods) [4, 5], based on the concept of absorbing boundary conditions [3], are particularly well suited for such problems. The present study aims at finding efficient transmission conditions in the case of the coupling between two diffusion equations representing the turbulent vertical mixing in the planetary boundary layers near the air-sea interface (see section 3.1 for further details on the notion of turbulent vertical mixing).

In the first part of this paper [9], we derive analytically optimized conditions in the case of a diffusion coefficient constant in each medium but with a discontinuity through the interface. However, this provides only a simplified view of the true physics. The ocean and the atmosphere interact through various multi-scale physical processes that are usually hardly explicitly resolved by the spatio-temporal discretization. Because it is essential to account for the effect of the subgrid turbulent boundary layers on the resolved part of the flow, parameterization schemes have been designed [7, 14]. Those schemes usually take the form

---

\*Corresponding author, Institute of Geophysics and Planetary Physics, University of California at Los Angeles, 405 Hilgard Avenue, Los Angeles, CA 90024-1567, United States (florian@atmos.ucla.edu, phone : +1-310-8255402, fax : +1-310-206-3051).

†INRIA Grenoble Rhône-Alpes, Montbonnot, 38334 Saint Ismier Cedex, France and Jean Kuntzmann Laboratory, BP 53, 38041 Grenoble Cedex 9, France (laurent.debreu@imag.fr, phone : +33 4 76 51 48 60, fax : +33 4 76 63 12 63).

‡University of Grenoble, Jean Kuntzmann Laboratory, BP 53, 38041 Grenoble Cedex 9, France (eric.blayo@imag.fr, phone : +33 4 76 63 59 63, fax : +33 4 76 63 12 63).

of a turbulent mixing term with a spatially variable diffusion coefficient to account for local effects. Indeed, a parameterization with a constant diffusion, originally introduced in [2], is now known to be naive. In this second part of the paper, we intend to study the impact of this variability of the diffusion coefficients, in particular in the vicinity of the interface, on the convergence properties of the Schwarz algorithm. To our knowledge, the spatial variability of the coefficients has never been considered in the framework of Schwarz-like methods, except in [10] where absorbing conditions are given for a one-dimensional stationary diffusion problem.

This paper is organized as follows. In the rest of this section, we briefly recall the aspects of optimized Schwarz methods necessary to understand the problematic of the present study. In section 2, we introduce a general methodology to analytically assess the impact of the spatial variability of diffusion coefficients on the convergence of the Schwarz method. This method is applied first to a simple *Dirichlet-Neumann* algorithm and then to a more general *Robin-Robin* algorithm. Finally, in section 3, we illustrate the relevancy of our approach with numerical results.

**1.2. Model problem and Schwarz algorithm.** The present study focuses on the coupling between two one-dimensional diffusion equations with variable coefficients. Let  $\Omega_1 = ]-L_1, 0[$  and  $\Omega_2 = ]0, L_2[$  be two subdomains with a common interface  $\Gamma = \{x = 0\}$ . The coupling problem reads

$$(1.1) \quad \begin{cases} \mathcal{L}_1 u_1 = f & \text{in } \Omega_1 \times [0, T] \\ u_1(x, 0) = u_o(x) & x \in \Omega_1 \\ \mathcal{B}_1 u_1(-L_1, t) = g_1 & t \in [0, T] \\ \mathcal{F}_1 u_1(0, t) = \mathcal{F}_2 u_2(0, t) & \text{on } \Gamma \times [0, T] \end{cases} \quad \begin{cases} \mathcal{L}_2 u_2 = f & \text{in } \Omega_2 \times [0, T] \\ u_2(x, 0) = u_o(x) & x \in \Omega_2 \\ \mathcal{B}_2 u_2(L_2, t) = g_2 & t \in [0, T] \\ \mathcal{G}_2 u_2(0, t) = \mathcal{G}_1 u_1(0, t) & \text{on } \Gamma \times [0, T] \end{cases}$$

where  $\mathcal{L}_j = \partial_t - \partial_x(D_j(x)\partial_x)$ ,  $\mathcal{B}_j$  corresponds to the boundary conditions on the computational domain  $\Omega$ ,  $\mathcal{F}_j$  and  $\mathcal{G}_j$  are operators defining the interface conditions. Those operators must be designed to ensure a given consistency of the solution through  $\Gamma$ . In our study we require the equality of subproblems solutions and of their normal fluxes.

In order to solve the coupling problem (1.1), we propose to implement a Schwarz algorithm with *Robin-Robin* interface conditions :

$$(1.2) \quad \begin{cases} \mathcal{L}_1 u_1^k = f & \text{in } \Omega_1 \times [0, T] \\ u_1^k(x, 0) = u_o(x), & x \in \Omega_1 \\ \mathcal{B}_1 u_1^k(-L_1, t) = g_1 & t \in [0, T] \\ (D_1(0)\partial_x + \Lambda_1) u_1^k(0, t) = (D_2(0)\partial_x + \Lambda_1) u_2^{k-1}(0, t) & \text{on } \Gamma \times [0, T] \end{cases} \quad \begin{cases} \mathcal{L}_2 u_2^k = f & \text{in } \Omega_2 \times [0, T] \\ u_2^k(x, 0) = u_o(x) & x \in \Omega_2 \\ \mathcal{B}_2 u_2^k(L_2, t) = g_2 & t \in [0, T] \\ (-D_2(0)\partial_x + \Lambda_2) u_2^k(0, t) = (-D_1(0)\partial_x + \Lambda_2) u_1^k(0, t) & \text{on } \Gamma \times [0, T] \end{cases}$$

where  $k = 1, 2, \dots$  is the iteration number and the initial guess  $u_2^0(0, t)$  is given.  $\Lambda_1$  and  $\Lambda_2$  are operators to be determined. As mentioned in [10], those operators can be either local or nonlocal.

**1.3. Reminder of the framework in the case of constant (but discontinuous) diffusion coefficients.** We recall briefly here some known results useful for the present study and detailed in [9]. The convergence study of algorithm (1.2) with constant coefficients is performed by introducing the errors  $e_j^k = u_j^k - u^*$  between the  $k$ -th iterate and the exact solution

$u^*$  of the coupled problem. Using a Fourier transform in time (denoted for any function  $g \in L^2(\mathbb{R})$  by  $\widehat{g} := \mathcal{F}g$ ), the partial differential equation  $\mathcal{L}_j e_j = 0$  becomes an ordinary differential equation  $\widehat{\mathcal{L}}_j \widehat{e}_j = i\omega \widehat{e}_j - D_j \frac{\partial^2 \widehat{e}_j}{\partial x^2} = 0$  ( $D_j$  is spatially constant here) whose characteristic roots are :

$$\sigma_j^+ = \sqrt{\frac{i\omega}{D_j}}, \quad \sigma_j^- = -\sigma_j^+ = -\sqrt{\frac{i\omega}{D_j}}.$$

It is then usually assumed that  $L_j \rightarrow \infty$  and that  $e_j$  tends to zero for  $x \rightarrow \infty$  which leads to

$$\widehat{e}_1^k(x, \omega) = \alpha^k(\omega) e^{\sigma_1^+ x} \quad \widehat{e}_2^k(x, \omega) = \beta^k(\omega) e^{\sigma_2^- x}$$

where  $\alpha(\omega)$  and  $\beta(\omega)$  are determined to satisfy the boundary conditions. Finally the convergence factor  $\rho$  corresponding to the ratio between the errors at two successive iterations can be determined as a function of  $\sigma_j^\pm, D_j$  and  $\lambda_j$  (the Fourier symbols of the  $\Lambda_j$  operators):

$$(1.3) \quad \rho = \left| \frac{(\lambda_1(\omega) + D_2 \sigma_2^-) (\lambda_2(\omega) - D_1 \sigma_1^+)}{(\lambda_1(\omega) + D_1 \sigma_1^+) (\lambda_2(\omega) - D_2 \sigma_2^-)} \right|$$

We remark that in the Fourier space the following symbols

$$\lambda_1^{\text{opt}} = -D_2 \sigma_2^- \quad \lambda_2^{\text{opt}} = D_1 \sigma_1^+$$

lead to  $\rho = 0$ , i.e. ensure a convergence in exactly two iterations. However the corresponding operators, which are called *absorbing* conditions, are nonlocal in time, and therefore cannot be used in practical applications. We thus need to look for a local approximation of these optimal operators. It has first been suggested in [11] to use a low frequency approximation of the symbols based on a Taylor expansion about  $\omega = 0$ . This results in effective transmission conditions only for  $\omega$  small. To obtain a more general approximation, efficient also for high frequencies, the so called *Optimized Schwarz Methods* (OSM) have been introduced. The simplest version consists in approximating  $\lambda_1^{\text{opt}}$  and  $\lambda_2^{\text{opt}}$  by two constant values  $\lambda_1^0$  and  $\lambda_2^0$ : this corresponds to Robin interface conditions (also called zeroth order *two-sided* transmission conditions). The values for  $\lambda_1^0$  and  $\lambda_2^0$  are then determined by solving the optimization problem

$$(1.4) \quad \min_{\lambda_1^0, \lambda_2^0 \in \mathbb{R}} \left( \max_{\omega \in [\omega_{\min}, \omega_{\max}]} \rho(\lambda_1, \lambda_2, \omega) \right)$$

In [9] this optimization problem is solved analytically for constant (and possibly discontinuous across  $\Gamma$ ) diffusion coefficients. In this second part of our study, we complement the preceding work [9] and discuss the effect of the spatial variability of the diffusion coefficients on the convergence speed and on the determination of optimized conditions.

When the diffusion coefficient is spatially variable the usual approach in determining the convergence factor is no longer straightforward. To circumvent this problem, we develop in the next section a methodology to find analytically a way to derive a convergence factor, similar to (1.3), but including the spatial variability of the diffusion coefficients. Thanks to this new convergence factor, it will then be possible to solve numerically the min-max problem (1.4) to find optimal  $\lambda_j^0$  values. We expect a non-trivial effect of this variability on the convergence properties of the associated Schwarz algorithm. Indeed, in [10] it is shown, for the stationary

diffusion equation  $-\partial_x (D(x)\partial_x u) = f$ , that the absorbing conditions are given by Robin conditions with  $\lambda_1^{\text{opt}} = \left( \int_{-L_1}^0 D_1^{-1}(s) ds \right)^{-1}$  and  $\lambda_2^{\text{opt}} = \left( \int_0^{L_2} D_2^{-1}(s) ds \right)^{-1}$ . This result strongly suggests that this is not only the local values of the diffusion coefficient near the interface that have an impact on the  $\lambda_j$  parameters but the whole profile  $D(x)$  all over  $\Omega$ .

**2. OSM for diffusion problems with spatially variable coefficients.** As mentioned previously, the diffusion coefficient may be spatially variable to account for local effects (e.g., in the turbulent boundary layers) within subdomains. In practical applications (like in oceanography or meteorology) diffusion coefficients are likely to vary by several orders of magnitude in the vertical direction (this point is further discussed in section 3.1). That is the primary motivation to look for a methodology to determine analytically the convergence factor for non constant diffusion coefficients defined on two non-overlapping subdomains. Throughout this study we make the assumption that the diffusion profile does not vary with time.

**2.1. Analytical determination of the shape of the errors.** The first part of this section does not require any distinction between subdomains, so the  $j$  subscripts are temporarily dropped. We denote by  $g(t)$  the function containing the information given by the neighboring subdomain, the problem under investigation is

$$(2.1) \quad \begin{cases} \partial_t e - \partial_x (D(x) \partial_x e) = 0 & x \in ]0, L[, t > 0 \\ e(x, 0) = 0 & x \in ]0, L[ \\ -D(0) \partial_x e(0, t) + \lambda e(0, t) = g(t) & t > 0 \\ e(L, t) = 0 & t > 0 \end{cases}$$

with  $\lambda$  the Robin parameter we wish to determine to optimize the convergence speed. A Dirichlet condition is imposed at  $x = L$ , this corresponds in having  $\mathcal{B}_1 = \mathcal{B}_2 = \text{I}$  in (1.2), with I the identity map.

First, we notice that the method based on a Fourier analysis, commonly used to analytically determine the convergence factor, is less convenient for our model problem with variable coefficients. Indeed, in Fourier space, we would obtain the ODE  $i\omega \hat{e} - \partial_x (D(x)\partial_x \hat{e}) = 0$  for  $\hat{e}$ . The study of this ODE appears to be at least as complicated as the original problem in physical space. That is why we propose to study directly the system (2.1). We transform this original problem with a homogeneous equation and nonhomogeneous boundary conditions into a problem with nonzero right-hand side but with homogeneous boundary conditions, by searching for a solution under the form  $e(x, t) = \varphi(x, t) + U(x, t)$  with  $\varphi$  a lifting function satisfying the boundary conditions. The transformed problem reads

$$(2.2) \quad \begin{cases} \partial_t U - \partial_x (D(x) \partial_x U) = f(x, t) = -\partial_t \varphi + \partial_x (D(x) \partial_x \varphi) & x \in ]0, L[, t > 0 \\ U(x, 0) = -\varphi(x, 0) & x \in ]0, L[ \\ -D(0) \partial_x U(0, t) + \lambda U(0, t) = 0 & t > 0 \\ U(L, t) = 0 & t > 0 \end{cases}$$

The choice of  $\varphi$  is not unique. We choose this function as the solution of problem (2.1) with a constant diffusion coefficient whose value is the value at  $x = 0$ ; i.e.,  $\varphi$  is solution of

$$(2.3) \quad \begin{cases} \partial_t \varphi - D(0) \partial_{xx} \varphi = 0 & x \in ]0, L[, t > 0 \\ -D(0) \partial_x \varphi(0, t) + \lambda \varphi(0, t) = g(t) & t > 0 \\ \varphi(L, t) = 0 & t > 0 \end{cases}$$

We then search for  $U(x, t)$  using a separation of variables  $U(x, t) = \sum_n \Phi_n(x) T_n(t)$ . Substitution in (2.2) leads to

$$\sum_n T_n'(t) \Phi_n(x) - \sum_n T_n(t) \partial_x (D(x) \partial_x \Phi_n(x)) = f(x, t),$$

where the right hand side is also expanded with respect to the functions  $\Phi_n(x)$

$$f(x, t) = -\partial_t \varphi + \partial_x (D(x) \partial_x \varphi) = \sum_n f_n(t) \Phi_n(x)$$

The next step is to properly choose the  $\Phi_n$ s. An adequate choice would enable us to transform the PDE into ODEs for unknown functions  $\Phi_n(x)$  and  $T_n(t)$ . The natural choice is therefore to look for  $\Phi_n(x)$  as a solution of the following *regular Sturm-Liouville* (SL) problem

$$(2.4) \quad \begin{cases} \partial_x (D(x) \partial_x \Phi_n) + c_n^2 \Phi_n = 0 & x \in ]0, L[ \\ -D(0) \partial_x \Phi_n(0) + \lambda \Phi_n(0) = 0 \\ \Phi_n(L) = 0 \end{cases}$$

with  $c_n$  the eigenvalues of the SL operator. Such a choice leads to a family of functions  $\Phi_n(x)$  which are orthonormal for the Euclidian scalar product  $\langle u, v \rangle = \int_0^L u(x)v(x)dx$ . The properties of regular SL problems are fully described in [1] or [6]. After some simple algebra we find that a general solution of problem (2.1) is given by

$$(2.5) \quad e(x, t) = \varphi(x, t) + U(x, t)$$

with  $U(x, t) = \sum_n \Phi_n(x) \int_0^t \exp(-c_n^2(t-\tau)) f_n(\tau) d\tau$ . In (2.5),  $\varphi$  satisfies (2.3),  $\Phi_n$  satisfies (2.4) and  $f_n(t)$  satisfies

$$f_n(t) = \int_0^L \partial_x (\tilde{D}(x) \partial_x \varphi) \Phi_n(x) dx \quad \text{with } \tilde{D}(x) = D(x) - D(0)$$

By formulating the solution of our problem under this form we can properly separate the error into two parts corresponding to two different contributions:  $\varphi(x, t)$  corresponds to the error for a constant coefficient  $D(0)$ , and  $U(x, t)$  represents the error coming from the perturbations around  $D(0)$ , namely  $\tilde{D}(x)$ .

We must now determine explicitly the function  $\varphi$ . A straightforward way consists in using the continuous Fourier transform in time. By introducing the function  $E_\omega(x) = e^{\sqrt{\frac{i\omega}{D(0)}}x}$  and by taking into account the boundary conditions at  $x = 0$  and  $x = L$ , we get

$$\hat{\varphi}(x, \omega) = \frac{E_\omega(x) - E_\omega(2L - x)}{\lambda(1 - E_\omega(2L)) - \sqrt{i\omega D(0)}(1 + E_\omega(2L))} \hat{g}(\omega)$$

It is now possible to express the error (2.5) in the Fourier space. The  $f_n$  functions are extended by zero for  $t < 0$  and by the convolution theorem we have

$$\mathcal{F} \left\{ \int_0^t \exp(-c_n^2(t-\tau)) f_n(\tau) d\tau \right\} = \hat{s}_n(\omega) \hat{f}_n(\omega) \quad \text{with } \hat{s}_n(\omega) = \mathcal{F} \left( e^{-c_n^2 t} H(t) \right) = \frac{1}{c_n^2 + i\omega}$$

where  $H(t)$  is the Heaviside unit step function. The general form for  $\widehat{e}(x, \omega)$  is

$$\widehat{e}(x, \omega) = \widehat{\varphi}(x, \omega) + \sum_n \Phi_n(x) \widehat{s}_n(\omega) \widehat{f}_n(\omega)$$

In practice it is usually assumed that the subdomains are unbounded ( $L \rightarrow \infty$ ) to simplify the expression of the convergence factor and thus to simplify the optimization problem (1.4). Using this assumption,  $\widehat{\varphi}$  becomes

$$\widehat{\varphi}(x, \omega) \simeq \frac{E_\omega(-x)}{\lambda + \sqrt{i\omega D(0)}} \widehat{g}(\omega),$$

which implies

$$\widehat{f}_n(\omega) \simeq \frac{\widehat{g}(\omega)}{\lambda + \sqrt{i\omega D(0)}} \int_0^L \frac{\partial}{\partial x'} \left( \widetilde{D}(x') \frac{\partial}{\partial x'} E_\omega(-x') \right) \Phi_n(x') dx'$$

As a result of our study we come up with an expression for the error function in Fourier space that takes into account the spatial variability of the diffusion coefficient:

(2.6)

$$\widehat{e}(x, \omega) \simeq \frac{\widehat{g}(\omega)}{\lambda + \sqrt{i\omega D(0)}} \left[ E_\omega(-x) + \sum_n \frac{\sqrt{\frac{i\omega}{D(0)}} \Phi_n(x)}{i\omega + c_n^2} \int_0^L \widetilde{D}(x') E_\omega(-x') \frac{d\Phi_n}{dx'} dx' \right] \quad x \geq 0$$

This error has been constructed for positive values of  $x$  which can be identified to subdomain  $\Omega_2$ , following the notations introduced in section 1.2. For  $x$  negative (i.e., on  $\Omega_1$ ), we obtain a very similar form:

(2.7)

$$\widehat{e}(x, \omega) \simeq \frac{\widehat{h}(\omega)}{\lambda + \sqrt{i\omega D(0)}} \left[ E_\omega(x) - \sum_n \frac{\sqrt{\frac{i\omega}{D(0)}} \Phi_n(x)}{i\omega + c_n^2} \int_{-L}^0 \widetilde{D}(x') E_\omega(x') \frac{d\Phi_n}{dx'} dx' \right] \quad x \leq 0$$

where the function  $h$  is the analogous of function  $g$  previously introduced.

The form (2.6) of the error suggests that the impact of the spatial variability of the diffusion coefficients will be primarily seen for low temporal frequencies. Indeed, the term  $\widetilde{D}(x)$  arising from the variability of the coefficient is weighted by  $|E_\omega(-x)| = e^{-\sqrt{\frac{i\omega}{2\widetilde{D}(0)}}x}$ , making the effect of the variability negligible for large values of  $\omega$  but potentially significant for low frequencies. Moreover we can draw the same remark for the variations with  $x$ : when  $x$  is small (near the interface)  $\widetilde{D}(x)$  is weighted by a non negligible number while for  $x$  large enough  $E_\omega(-x)$  is very small.

**2.2. Convergence factor of the Dirichlet-Neumann algorithm with spatially variable coefficients.** We have established so far a general form for the errors propagating in each subdomain. We are now able to propose a formulation of the convergence speed for the global-in-time Schwarz algorithm with spatially variable coefficients. Before dealing with the general Robin-Robin case we intend to determine the convergence speed in a simpler Dirichlet-Neumann case; i.e., with the notations introduced in (1.1),  $\mathcal{G}_j = \text{I}$  and  $\mathcal{F}_j = D_j(0) \frac{\partial}{\partial x}$ . Moreover, for sake of practical convenience, we also try to find the expression of an "effective" value  $D_j^{\text{eff}}$  corresponding to a constant value that would have the same effect on the convergence speed than the whole non constant diffusion profile  $D_j(x)$ . Hereafter

we use again the subscripts  $j$  to characterize both subdomains and we introduce the function  $E_{\omega,j}(x) = e^{\sqrt{\frac{i\omega}{D_j(0)}}x}$  that plays the same role than the  $E_\omega$  function previously defined.

A derivation very similar to what has been done in section 2.1, but with a Dirichlet boundary condition instead of a Robin boundary condition leads to:

$$(2.8) \quad \widehat{e}_2(x, \omega) = \left( E_{\omega,2}(-x) + \sum_n \frac{\Phi_{n,2}(x) \sqrt{\frac{i\omega}{D_2(0)}}}{i\omega + c_{n,2}^2} \int_0^{L_2} \widetilde{D}_2(x') E_{\omega,2}(-x') \frac{d\Phi_{n,2}}{dx'}(x') dx' \right) \widehat{g}(\omega)$$

where  $\widehat{g}(\omega) = \widehat{e}_1(0, \omega)$  and where the  $\Phi_{n,2}$  are defined by a SL problem similar to (2.4), but again with a Dirichlet condition instead of a Robin condition. On  $\Omega_1$ , we have (by simply making  $\lambda = 0$  in the derivation of section 2.1):

$$(2.9) \quad \widehat{e}_1(x, \omega) = \left( E_{\omega,1}(x) - \sum_n \frac{\Phi_{n,1}(x) \sqrt{\frac{i\omega}{D_1(0)}}}{i\omega + c_{n,1}^2} \int_{-L_1}^0 \widetilde{D}_1(x') E_{\omega,1}(x) \frac{d\Phi_{n,1}}{dx'}(x') dx' \right) \frac{\widehat{h}(\omega)}{\sqrt{i\omega D_1(0)}}$$

where  $\widehat{h}(\omega) = D_2(0) \frac{\partial \widehat{e}_2}{\partial x}(0, \omega)$  and where the  $\Phi_{n,1}$  are defined by a SL problem similar to (2.4) with a homogeneous Neumann condition at  $x = 0$ . The multiplicative Schwarz algorithm with Dirichlet-Neumann conditions is obtained by replacing  $\widehat{e}_2$  (resp.  $\widehat{g}$ ) by  $\widehat{e}_2^k$  (resp.  $\widehat{e}_1^k(0, \omega)$ ) in (2.8), and  $\widehat{e}_1$  (resp.  $\widehat{h}$ ) by  $\widehat{e}_1^k$  (resp.  $\widehat{h}^{k-1}(\omega) = D_2(0) \frac{\partial \widehat{e}_2^{k-1}}{\partial x}(0, \omega)$ ) in (2.9). Therefore we have:

$$\widehat{g}^k(\omega) = \left( 1 - \sum_n \frac{\Phi_{n,1}(0) \sqrt{\frac{i\omega}{D_1(0)}}}{i\omega + \lambda_{n,1}^2} \int_{-L_1}^0 \widetilde{D}_1(x') E_{\omega,1}(x') \frac{d\Phi_{n,1}}{dx'}(x') dx' \right) \frac{\widehat{h}^{k-1}(\omega)}{\sqrt{i\omega D_1(0)}}$$

$$\widehat{h}^k(\omega) = \left( -1 + \sum_n \frac{\frac{d\Phi_{n,2}}{dx}(0)}{i\omega + \lambda_{n,2}^2} \int_0^{L_2} \widetilde{D}_2(x') E_{\omega,2}(-x') \frac{d\Phi_{n,2}}{dx'}(x') dx' \right) \sqrt{i\omega D_2(0)} \widehat{g}^k(\omega)$$

Then, if we define a convergence factor by

$$\rho_{\text{DN}}^{\text{var}}(\omega) = \left| \frac{\widehat{e}_1^k(0, \omega)}{\widehat{e}_1^{k-1}(0, \omega)} \right|$$

the previous relations lead to

$$(2.10) \quad \rho_{\text{DN}}^{\text{var}}(\omega) = \left| \frac{\widehat{g}^k}{\widehat{g}^{k-1}} \right| = \left| \frac{\widehat{g}^k}{\widehat{h}^{k-1}} \frac{\widehat{h}^{k-1}}{\widehat{g}^{k-1}} \right| = \rho_{\text{DN}}^{\text{cst}} \cdot \widetilde{\rho}_{\text{DN}}$$

where  $\rho_{\text{DN}}^{\text{cst}} = \sqrt{\frac{D_2(0)}{D_1(0)}}$  is the convergence factor obtained in the case of constant diffusion coefficients (see [12]) and

$$\widetilde{\rho}_{\text{DN}} = \left| \left( 1 - \sum_n \frac{\sqrt{\frac{i\omega}{D_1(0)}} \Phi_{n,1}(0)}{i\omega + c_{n,1}^2} \int_{-L_1}^0 \widetilde{D}_1(x') E_{\omega,1}(x') \frac{d\Phi_{n,1}}{dx'}(x') dx' \right) \left( 1 - \sum_n \frac{\frac{d\Phi_{n,2}}{dx}(0)}{i\omega + c_{n,2}^2} \int_0^{L_2} \widetilde{D}_2(x') E_{\omega,2}(-x') \frac{d\Phi_{n,2}}{dx'}(x') dx' \right) \right|$$

This result shows that the convergence factor  $\rho_{\text{DN}}^{\text{var}}$  naturally appears as the product of the convergence factor with constant coefficients (the surface values) by a term coming from the spatial variability of the diffusion coefficient on  $\Omega_1$  and  $\Omega_2$ .

Starting from equation (2.10) we can suggest two "effective" constant values for  $D_1$  and  $D_2$ . Those (spatially constant) values would have a similar effect on the convergence speed than the non constant vertical profiles  $D_1(x)$  and  $D_2(x)$ , they would satisfy  $\rho_{\text{DN}}^{\text{var}} = \sqrt{\frac{D_2^{\text{eff}}(\omega)}{D_1^{\text{eff}}(\omega)}}$  with

$$D_1^{\text{eff}}(\omega) = \frac{D_1(0)}{\left| 1 - \sum_n \frac{\sqrt{\frac{i\omega}{D_1(0)} \Phi_{n,1}(0)}}{i\omega + c_{n,1}^2} \int_{-L_1}^0 \tilde{D}_1(x') E_{\omega,1}(x') \frac{d\Phi_{n,1}(x')}{dx'} dx' \right|^2}$$

and respectively

$$D_2^{\text{eff}}(\omega) = D_2(0) \left| 1 - \sum_n \frac{\frac{d\Phi_{n,2}(0)}{dx}}{i\omega + c_{n,2}^2} \int_0^{L_2} \tilde{D}_2(x') E_{\omega,2}(-x') \frac{d\Phi_{n,2}(x')}{dx'} dx' \right|^2$$

It is worth mentioning that, due to the variability of the coefficients, the convergence factor is a function of the time frequency  $\omega$  whereas this dependency does not exist with constant coefficients. Some examples of convergence factors  $\rho_{\text{DN}}^{\text{var}}$  are given in section 3.2. Note that in the case  $\omega \rightarrow 0$  we get  $D_1^{\text{eff}} \rightarrow D_1(0)$  while

$$D_2^{\text{eff}}(\omega \rightarrow 0) = D_2(0) \left| 1 - \sum_n c_{n,2}^{-2} \frac{d\Phi_{n,2}(0)}{dx} \int_0^{L_2} \tilde{D}_2(x') \frac{d\Phi_{n,2}(x')}{dx'} dx' \right|^2$$

The effect of the variability of the coefficient in the subdomain with a Neumann condition asymptotically vanishes. This is however not the case for the subdomain  $\Omega_2$  with Dirichlet conditions. This suggests that depending on  $\tilde{D}_2(x)$ , and associated  $c_{n,2}$  and  $\Phi_{n,2}$ , nothing ensures that  $\rho_{\text{DN}}^{\text{cst}} < 1$  implies  $\rho_{\text{DN}}^{\text{var}} < 1$  when a Dirichlet-Neumann algorithm is used. Indeed

$$(2.11) \quad \rho_{\text{DN}}^{\text{var}}(\omega \rightarrow 0) \rightarrow \sqrt{\frac{D_2(0)}{D_1(0)}} \left( 1 - \sum_n c_{n,2}^{-2} \frac{d\Phi_{n,2}(0)}{dx} \int_0^{L_2} \tilde{D}_2(x') \frac{d\Phi_{n,2}(x')}{dx'} dx' \right)$$

whereas  $\rho_{\text{DN}}^{\text{var}}(\omega \rightarrow \infty) \rightarrow \rho_{\text{DN}}^{\text{cst}}$ .

**2.3. Convergence factor of the Robin-Robin algorithm with spatially variable coefficients.** In this section we determine the convergence factor  $\rho_{\text{RR}}^{\text{var}}$  in the more general case of Robin-Robin interface conditions. Thanks to (2.6) and (2.7), we can express  $\hat{e}_1$  and  $\hat{e}_2$  in a compact form for iterate  $k$  :

$$(2.12) \quad \begin{cases} \hat{e}_1^k(\omega, 0) = \mathcal{K}_1(\omega, D_1(0), \Phi_{n,1}, c_{n,1}, \lambda_1) \hat{h}^{k-1} \\ \hat{e}_2^k(\omega, 0) = \mathcal{K}_2(\omega, D_2(0), \Phi_{n,2}, c_{n,2}, \lambda_2) \hat{g}^k \end{cases}$$

where  $\hat{g} = -D_1(0)\partial_x \hat{e}_1(0, \omega) + \lambda_2 \hat{e}_1(0, \omega)$ ,  $\hat{h} = D_2(0)\partial_x \hat{e}_2(0, \omega) + \lambda_1 \hat{e}_2(0, \omega)$ , and

$$\begin{cases} \mathcal{K}_1 = \left( 1 - \sum_n \frac{\sqrt{\frac{i\omega}{D_1(0)} \Phi_{n,1}(0)}}{i\omega + c_{n,1}^2} \int_{-L_1}^0 \tilde{D}_1(x') E_{\omega,1}(x') \frac{d\Phi_{n,1}(x')}{dx'} dx' \right) \frac{1}{\lambda_1 + \sqrt{i\omega D_1(0)}} \\ \mathcal{K}_2 = \left( 1 + \sum_n \frac{\sqrt{\frac{i\omega}{D_2(0)} \Phi_{n,2}(0)}}{i\omega + c_{n,2}^2} \int_0^{L_2} \tilde{D}_2(x') E_{\omega,2}(-x') \frac{d\Phi_{n,2}(x')}{dx'} dx' \right) \frac{1}{\lambda_2 + \sqrt{i\omega D_2(0)}} \end{cases}$$

The problem on the interface  $x = 0$  is given by the relations

$$(2.13) \quad \begin{cases} (D_1(0)\partial_x + \lambda_1)\widehat{e}_1^k(0, \omega) = (D_2(0)\partial_x + \lambda_1)\widehat{e}_2^{k-1}(0, \omega) = \widehat{h}^{k-1} \\ (-D_2(0)\partial_x + \lambda_2)\widehat{e}_2^k(0, \omega) = (-D_1(0)\partial_x + \lambda_2)\widehat{e}_1^k(0, \omega) = \widehat{g}^k \end{cases}$$

and by combining (2.12) and (2.13) we get

$$\begin{cases} D_1(0)\partial_x\widehat{e}_1^k(0, \omega) = \widehat{h}^{k-1} - \lambda_1\widehat{e}_1^k(0, \omega) = (1 - \lambda_1\mathcal{K}_1)\widehat{h}^{k-1} \\ -D_2(0)\partial_x\widehat{e}_2^k(0, \omega) = \widehat{g}^k - \lambda_2\widehat{e}_2^k(0, \omega) = (1 - \lambda_2\mathcal{K}_2)\widehat{g}^k \end{cases}$$

By substituting those expressions in (2.13) we finally get a relation linking  $\widehat{g}$  and  $\widehat{h}$

$$\begin{cases} \widehat{g}^k = [(\lambda_1 + \lambda_2)\mathcal{K}_1 - 1]\widehat{h}^{k-1} \\ \widehat{h}^{k-1} = [(\lambda_1 + \lambda_2)\mathcal{K}_2 - 1]\widehat{g}^{k-1} \end{cases}$$

which leads to an expression for the convergence factor

$$(2.14) \quad \rho_{\text{RR}}^{\text{var}} = \left| \frac{\widehat{g}^k}{\widehat{g}^{k-1}} \right| = |[(\lambda_1 + \lambda_2)\mathcal{K}_1 - 1] \cdot [(\lambda_1 + \lambda_2)\mathcal{K}_2 - 1]|$$

We can note that this expression of the convergence factor is consistent with the expression (1.3) obtained in the case of constant (but discontinuous) coefficients. Indeed, if we set  $\widetilde{D}_1(x) = \widetilde{D}_2(x) = 0$  in (2.14), we have then  $\mathcal{K}_j = 1/\sqrt{i\omega D_j(0)}$  which leads to (1.3) because  $D_j\sigma_j^\pm = \pm\sqrt{i\omega D_j(0)}$ . A convenient formulation of  $\rho_{\text{RR}}^{\text{var}}$  dropping the imaginary notations can be found in appendix A. To conclude this section we look at the asymptotic behavior of  $\rho_{\text{RR}}^{\text{var}}$ , and we can easily find that

$$\rho_{\text{RR}}^{\text{var}}(\omega \rightarrow 0) = \rho_{\text{RR}}^{\text{var}}(\omega \rightarrow \infty) \rightarrow 1$$

which shows that the effect of the variability of the diffusion coefficients asymptotically vanishes when a Robin-Robin algorithm is used.

**3. Numerical results.** In this section we check numerically the validity of the theoretical results presented in section 2. To do this, we first briefly describe the rationale for the spatial variability of the diffusion coefficient and provide a typical profile we will use for the numerical tests. Then we design a few experiments to illustrate the relevancy of our approach.

**3.1. Planetary boundary layer turbulence.** Unlike boundary layers in many engineering flows, the atmospheric and oceanic planetary boundary layers are almost always turbulent and cannot be explicitly resolved due to the insufficient vertical resolution in computational models. The numerical representation of those layers thus relies on the Reynolds decomposition: the flow is split into a mean (resolved) part  $\langle u \rangle$  and a fluctuating (subgrid) part  $u'$  (where  $u$  can either represent a velocity component or an active tracer). When this decomposition is applied to nonlinear (advective) terms this gives rise to additional terms and hence to a closure problem. The dominant term in the turbulent boundary layers arising from the Reynolds decomposition is the divergence of the vertical  $\langle u'w' \rangle$  term (where  $w$  denotes the vertical component of the velocity). Typically, this turbulent vertical flux is expressed as a function of the mean (resolved) part of the flow by using the *down-gradient assumption*,  $\langle u'w' \rangle = -D(x)\partial_x \langle u \rangle$  where  $D(x)$  is the so-called *eddy diffusivity*, or *eddy-viscosity* if  $u$  represents a velocity. This assumption explains why a one-dimensional diffusion equation, like the one studied in the present paper, is generally sufficient to locally represent the turbulent mixing in the boundary layers. The eddy diffusivity  $D(x)$  is defined to allow the flow

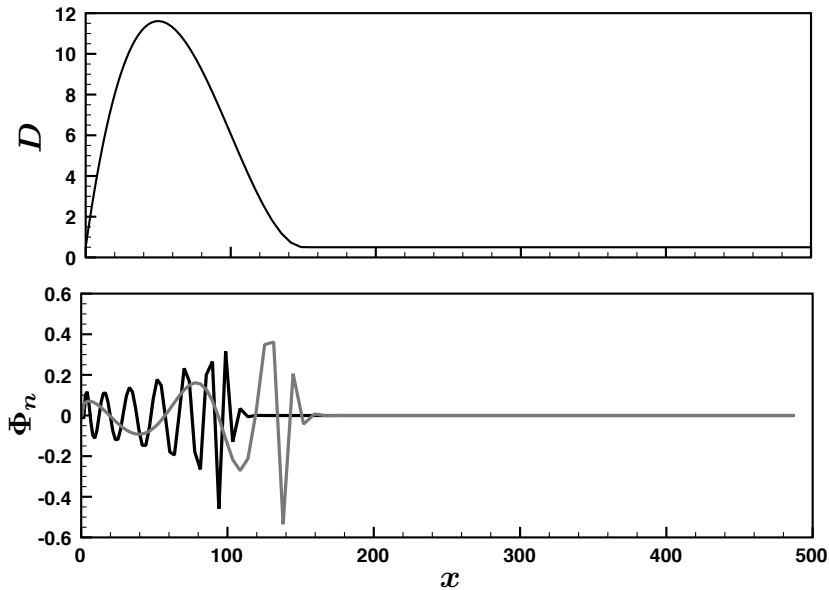


FIG. 3.1. Typical diffusion profile  $D(x)$  obtained for  $A = 0.5 \text{ m s}^{-1}$  and  $h_{bl} = 150 \text{ m}$  in (3.1) with respect to  $x$  (top), and two associated eigenfunctions  $\Phi_n(x)$  (bottom) of the Sturm-Liouville problem (2.4) with homogeneous Dirichlet condition at  $x = 0$ .

to make the transition between its surface (the air-sea interface) and its interior (below the boundary layer) properties. This is the reason why  $D(x)$  exhibits a strong spatial variability. In this context, several ways to specify the coefficient  $D(x)$  have been proposed. The most commonly used formulation in the state-of-the-art numerical models can be found in [7] and [14]. Those formulations define the eddy diffusivity as

$$(3.1) \quad D(x) = \begin{cases} A x \left(1 - \frac{x}{h_{bl}}\right)^2 + \nu & x \in ]0, h_{bl}] \\ \nu & x > h_{bl} \end{cases}$$

with  $h_{bl}$  the thickness of the boundary layer (depending on the state of the flow) and  $A$  a parameter setting the intensity of the mixing (note that  $D(x)$  is continuous and differentiable at  $x = h_{bl}$ ). Throughout this section we consider that  $D(x)$  is given by (3.1), and a typical profile for  $A = 0.5 \text{ m s}^{-1}$  and  $h_{bl} = 150 \text{ m}$  is given in Fig. 3.1.

In the remainder of this section we study first a Dirichlet-Neumann algorithm and then a Robin-Robin algorithm. We define spatially variable coefficients with  $A_1 = 0.1 \text{ m s}^{-1}$  (resp.  $A_2 = 0.5 \text{ m s}^{-1}$ ) and  $h_{bl,1} = 50 \text{ m}$  (resp.  $h_{bl,2} = 150 \text{ m}$ ) on  $\Omega_1$  (resp.  $\Omega_2$ ). The values of  $\nu_1$  and  $\nu_2$  (corresponding to the surface values  $D_1(0)$  and  $D_2(0)$ ) are chosen to be the same than the values used in [9] in the constant coefficient case. If we introduce  $\gamma = \sqrt{\frac{\nu_2}{\nu_1}}$ , we investigate the two cases  $\gamma = 10$  and  $\gamma = \sqrt{\sqrt{10}}$  with  $\nu_2 = 0.5 \text{ m}^2 \text{ s}^{-1}$  ( $\nu_1$  is adjusted depending on the value of  $\gamma$ ). Those various parameter values lead to diffusion profiles that can be found in the atmospheric and oceanic boundary layers. The discretization of the problem, the computational grid, as well as the initial conditions are described in [9]

(section 5). We use  $\Delta t = 100$  s, and a random initial guess on the interface so that it contains a wide range of the temporal frequencies that can be resolved by the computational grid .

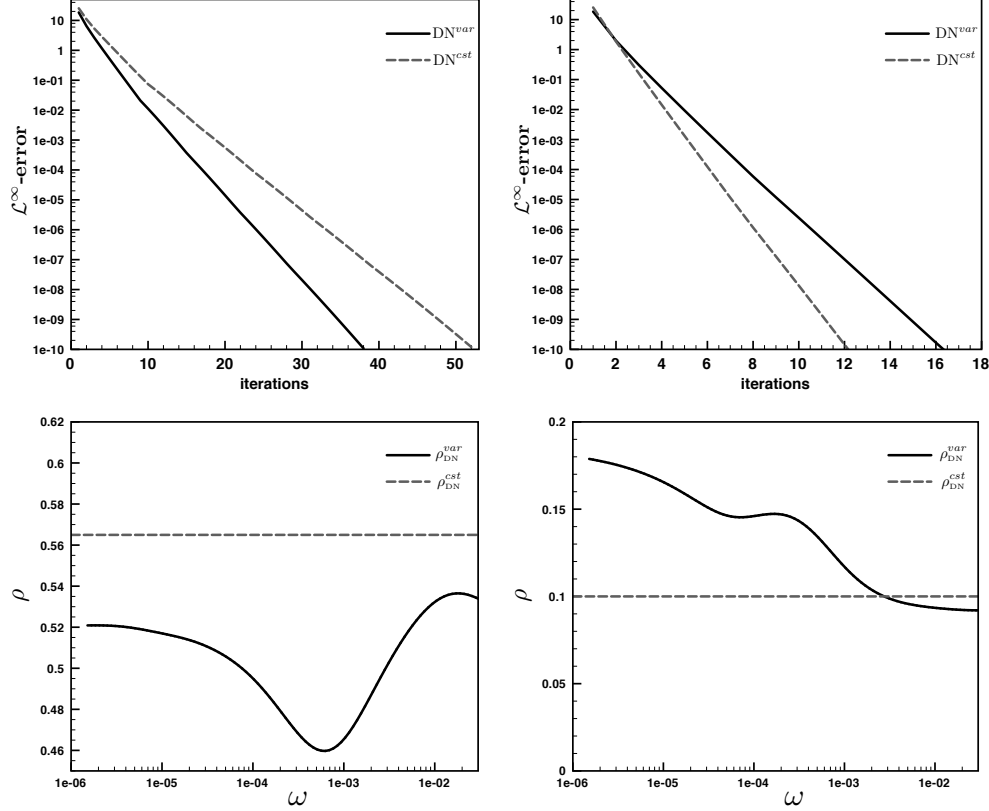


FIG. 3.2. Evolution of the  $L^\infty$ -norm of the error of the Dirichlet-Neumann algorithm as a function of the iterates for  $\gamma = \sqrt{\sqrt{10}}$  (top, left) and  $\gamma = 10$  (top, right). Those results are obtained for constant diffusion coefficients (gray dashed line) and for spatially variable coefficients (black line) as defined in Sec. 3.1. The corresponding convergence factors  $\rho_{\text{DN}}^{\text{var}}(\omega)$  (black line) and  $\rho_{\text{DN}}^{\text{est}}(\omega)$  (gray dashed line) determined at the analytical level are given for  $\gamma = \sqrt{\sqrt{10}}$  (bottom, left) and  $\gamma = 10$  (bottom, right).

**3.2. Testcase #1 : Dirichlet-Neumann.** The analytical convergence factor  $\rho_{\text{DN}}^{\text{var}}(\omega)$  (2.10) is shown for different values of  $\gamma$  in Fig. 3.2. The eigenvalues  $c_n$  and eigenfunctions  $\Phi_n$  are computed numerically on the same computational grid than the model problem. We remark that depending on the jump in the coefficients through the interface the spatial variability of the diffusivities either tend to accelerate the convergence speed (for  $\gamma = \sqrt{\sqrt{10}}$ ) or to slow it down (for  $\gamma = 10$ ) compared to the convergence speed obtained with constant coefficients. As expected, the convergence factor for spatially variable coefficients is no longer independent of  $\omega$ , and for low-frequencies we get a significant departure from the convergence rate of the algorithm with constant coefficients. The trend seen in the convergence factor  $\rho_{\text{DN}}^{\text{var}}(\omega)$  determined at a continuous level is confirmed by numerical results (Fig. 3.2, top panels). Those results, as well as the asymptotic expression (2.11), call for caution when we use a Dirichlet-Neumann algorithm with spatially variable coefficients because it can lead to per-

formances significantly different compared to the one obtained with constant coefficients. We can expect a Robin-Robin type algorithm to provide a more robust alternative thanks to the tuning of the  $\lambda_j$  parameters.

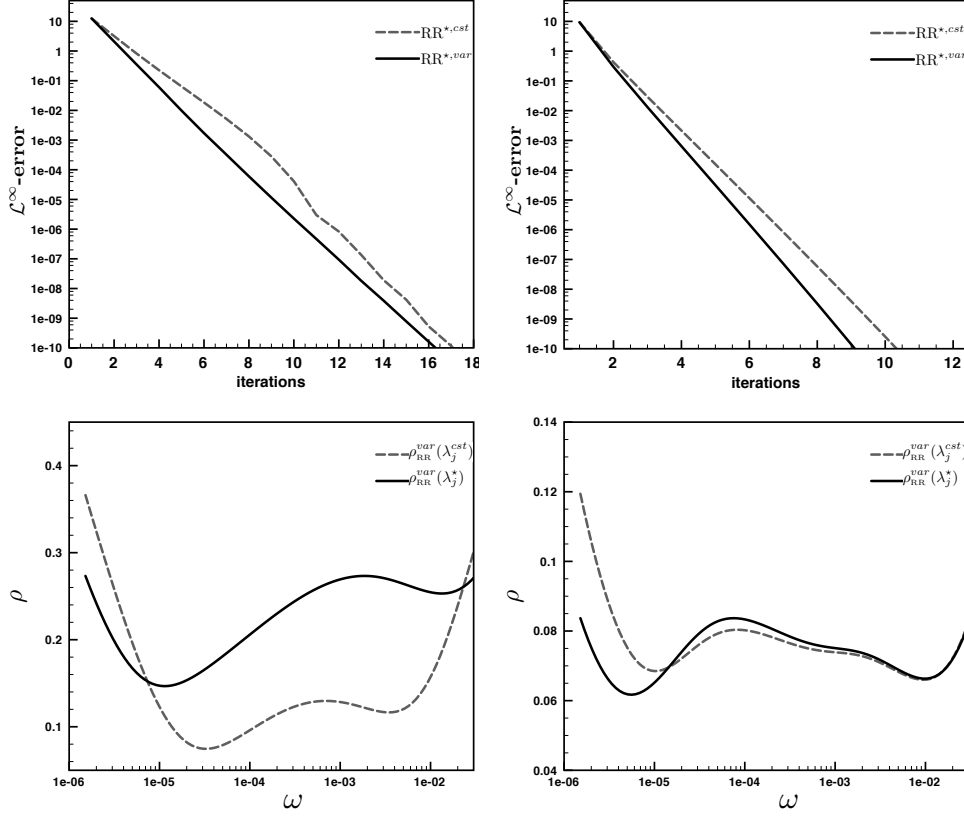


FIG. 3.3. Evolution of the  $L^\infty$ -norm of the error of the Robin-Robin algorithm as a function of the iterates for  $\gamma = \sqrt{10}$  (top, left) and  $\gamma = 10$  (top, right). Those results are obtained for spatially variable diffusion coefficients and the Robin parameters optimized by assuming constant coefficients (gray dashed line) or the full convergence factor  $\rho_{RR}^{\text{var}}$  (black line). The corresponding convergence factors  $\rho_{RR}^{\text{var}}(\lambda_j^*)$  (black line) and  $\rho_{RR}^{\text{var}}(\lambda_j^{\text{cst}})$  (gray dashed line) are given for  $\gamma = \sqrt{10}$  (bottom, left) and  $\gamma = 10$  (bottom, right).

**3.3. Testcase #2 : Robin-Robin.** In this paragraph, we note  $\lambda_j^{\text{cst}}$  the optimal Robin parameters obtained using the analytical results found in [9] for constant coefficients. We consider that those constant coefficients are the interface values  $D_j(0)$ . Moreover we note  $\lambda_j^{\text{var}}$  the Robin parameters optimized by solving numerically the problem (1.4) with the convergence factor  $\rho_{RR}^{\text{var}}$  as given in (2.14). This optimization is done using the Rosenbrock method [13] and by taking the  $\lambda_j^{\text{cst}}$  parameters to initialize the algorithm. We see from Fig. 3.3 that the use of the  $\lambda_j^{\text{var}}$  parameters provide slightly better convergence properties compared to the  $\lambda_j^{\text{cst}}$  parameters, whatever the value of  $\gamma$ . As for the Dirichlet-Neumann algorithm, we can check that our analytical study at the continuous level provides a convergence factor  $\rho_{RR}^{\text{var}}$  representative of the behavior of the algorithm at a discrete level (Fig. 3.3, bottom panels). From Fig. 3.3 (bottom left panel), we also see that the way we initialize the algorithm (with a random

initial guess for  $u_2^0(0, t)$ ,  $t \in [0, T]$ ) leads to the generation of a large range of temporal frequencies and more particularly low frequencies slowing down the convergence speed of the simulation using the  $\lambda_j^{\text{cst}}$  parameters although the latter provide a faster convergence than the  $\lambda_j^{\text{var}}$  parameters for most of the frequency spectrum. For our model problem, the use of the

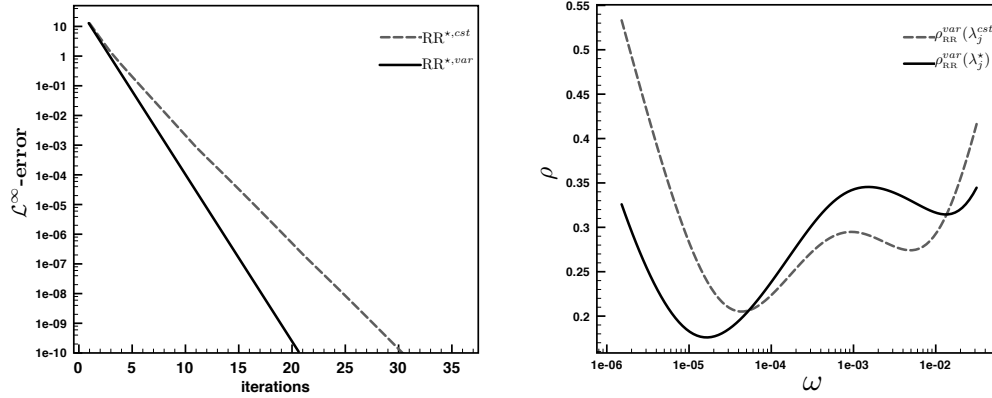


FIG. 3.4. Evolution of the  $\mathcal{L}^\infty$ -norm of the error (left) of the Robin-Robin algorithm as a function of the iterates for  $\gamma = \sqrt{\sqrt{10}}$  for  $h_{bl,2} = 10$  m (instead of  $h_{bl,2} = 150$  m as in Fig. 3.3). Those results are obtained for Robin parameters optimized by assuming constant coefficients (gray dashed line) or the full convergence factor  $\rho_{RR}^{\text{var}}$  (black line). The corresponding convergence factors  $\rho_{RR}^{\text{var}}(\lambda_j^*)$  (black line) and  $\rho_{RR}^{\text{var}}(\lambda_j^{\text{cst}})$  (gray dashed line) are on the right panel.

$\lambda_j^{\text{var}}$  parameters provides a relatively modest improvement over the  $\lambda_j^{\text{cst}}$  parameters. However, in general, this statement has to be mitigated because if we consider  $h_{bl,2} = 10$  m instead of  $h_{bl,2} = 150$  m we see in Fig. 3.4 that the parameters obtained through an optimization of  $\rho_{RR}^{\text{var}}$  are clearly superior to the  $\lambda_j^{\text{cst}}$  parameters. In the case we also show in Fig. 3.5 the asymptotic behaviour of the optimized convergence rate and associated Robin parameters  $\lambda_j^{\text{var}}$ . Provided some adjustments of the Robin parameters (those parameters can vary by several orders of magnitude with respect to  $\Delta t$ ), our algorithm asymptotically maintains a good efficiency.

**4. Conclusion.** We present and analyze in this paper a new approach to study the convergence properties of a global-in-time Schwarz algorithm in the case of a one-dimensional diffusion problem with spatially variable diffusion coefficients. We analytically derive an expression for the evolution of the errors of such an algorithm with respect to the iterates. Thanks to our formulation, we are able to gain a better understanding of the behavior of the associated convergence factor. We exhibit some interesting features that were not shown by usual convergence studies with constant diffusion coefficients. We put particular emphasis on the fact that for low temporal frequencies it can be a strong assumption to assimilate a variable diffusion coefficient to its constant interface value. Moreover we also show that depending on the type of algorithm under consideration (Dirichlet-Neumann or Robin-Robin) the variability of the coefficients may have more or less impact on the asymptotic convergence properties. To be more attractive for practical applications our approach requires further developments by performing an accurate study of the eigenvalues problem to improve our knowledge of the behavior of those eigenvalues with respect to the perturbations of the diffusion profiles.

**Acknowledgments.** This research was partially supported by the ANR project "COMMA" and by the INRIA project-team MOISE. The authors are thankful for the comments and suggestions of two anonymous reviewers, which helped to improve the clarity of this manuscript.

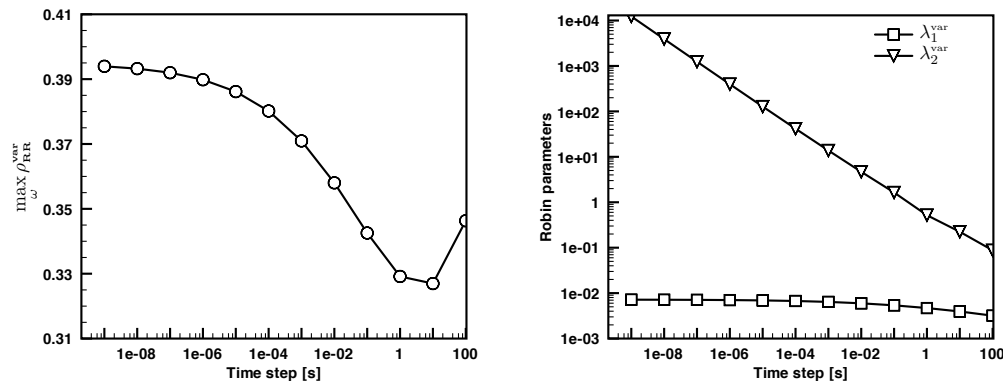


FIG. 3.5. Evolution of the convergence rate  $\max_{\omega} \rho_{RR}^{var}$  (left) and optimal Robin parameters  $\lambda_j^{var}$  (right) of the optimized Schwarz algorithm with spatially variable coefficients with respect to  $\Delta t$ . The parameters of the problem are  $h_{bl,1} = 50$  m,  $h_{bl,2} = 10$  m,  $A_1 = 0.1$  m s $^{-1}$ ,  $A_2 = 0.5$  m s $^{-1}$ , and  $\gamma = \sqrt{\sqrt{10}}$ .

#### REFERENCES

- [1] P. B. BAILEY, W. N. EVERITT, AND A. ZETTL, *Regular and singular Sturm-Liouville problems with coupled boundary conditions*, Proc. Roy. Soc. Edinburgh Sect. A, 126 (1996), pp. 505–514.
- [2] V. W. EKMAN, *On the influence of the earth's rotation on ocean currents*, Ark. Mat. Astron. Fys., 2 (1905), pp. 1–53.
- [3] B. ENGQUIST AND A. MAJDA, *Absorbing boundary conditions for the numerical simulation of waves*, Math. Comp., 31 (1977), pp. 629–651.
- [4] M. J. GANDER AND L. HALPERN, *Optimized Schwarz waveform relaxation methods for advection reaction diffusion problems*, SIAM J. Numer. Anal., 45 (2007), pp. 666–697 (electronic).
- [5] M. J. GANDER, L. HALPERN, AND F. NATAF, *Optimal convergence for overlapping and non-overlapping Schwarz waveform relaxation*, in Eleventh International Conference on Domain Decomposition Methods (London, 1998), DDM.org, Augsburg, 1999, pp. 27–36 (electronic).
- [6] Q. KONG AND A. ZETTL, *Eigenvalues of regular Sturm-Liouville problems*, J. Differential Equations, 131 (1996), pp. 1–19.
- [7] W. G. LARGE, J. C. MCWILLIAMS, AND S. C. DONEY, *Oceanic vertical mixing: A review and a model with a nonlocal boundary layer parameterization*, 32 (1994), pp. 363–403.
- [8] F. LEMARIÉ, *Algorithmes de Schwarz et couplage océan-atmosphère*, 2008. Thesis (Ph.D.)—Grenoble University (France).
- [9] F. LEMARIÉ, L. DEBREU, AND E. BLAYO, *Toward an optimized global-in-time schwarz algorithm for diffusion equations with discontinuous and spatially variable coefficients, part 1 : the constant coefficients case*, Electron. Trans. Numer. Anal., (2011). Under review.
- [10] P.-L. LIONS, *On the Schwarz alternating method. III. A variant for nonoverlapping subdomains*, in Third International Symposium on Domain Decomposition Methods for Partial Differential Equations (Houston, TX, 1989), SIAM, Philadelphia, PA, 1990, pp. 202–223.
- [11] F. NATAF, F. ROGIER, AND E. DE STURLER, *Optimal interface conditions for domain decomposition methods*, Internal Report 301, CMAP, 1994.
- [12] A. QUARTERONI AND A. VALLI, *Domain decomposition methods for partial differential equations*, Numerical Mathematics and Scientific Computation, The Clarendon Press Oxford University Press, New York, 1999. Oxford Science Publications.
- [13] H. H. ROSENBRUCK, *An automatic method for finding the greatest or least value of a function*, The Computer Journal, 3 (1960), pp. 175–184.
- [14] I. B. TROEN AND L. MAHRT, *A simple model of the atmospheric boundary layer; sensitivity to surface evaporation*, Boundary-Layer Meteorology, 37 (1986), pp. 129–148. 10.1007/BF00122760.

**Appendix A. Determination of the convergence factor in the case of variable coefficients.** We recall (2.14):

$$(A.1) \quad \rho = |[(\lambda_1 + \lambda_2)\mathcal{K}_1 - 1][(\lambda_1 + \lambda_2)\mathcal{K}_2 - 1]|$$

with

$$\begin{cases} \mathcal{K}_1 = \left( 1 - \sum_n \frac{\sqrt{\frac{i\omega}{D_1(0)}} \Phi_{n,1}(0)}{i\omega + \lambda_{n,1}^2} \int_{-L_1}^0 \tilde{D}_1(x) \exp\left(\sqrt{\frac{i\omega}{D_1(0)}} x\right) \frac{d\Phi_{n,1}}{dx} dx \right) \frac{1}{\lambda_1 + \sqrt{i\omega D_1(0)}} \\ \mathcal{K}_2 = \left( 1 + \sum_n \frac{\sqrt{\frac{i\omega}{D_2(0)}} \Phi_{n,2}(0)}{i\omega + \lambda_{n,2}^2} \int_0^{L_2} \tilde{D}_2(x) \exp\left(-\sqrt{\frac{i\omega}{D_2(0)}} x\right) \frac{d\Phi_{n,2}}{dx} dx \right) \frac{1}{\lambda_2 + \sqrt{i\omega D_2(0)}} \end{cases}$$

(A.1) can be rewritten as:

$$(A.2) \quad \rho = \sqrt{\left( \mathcal{I}m(\mathcal{K}_1)^2 (\lambda_1 + \lambda_2)^2 + [(\lambda_1 + \lambda_2)\mathcal{R}e(\mathcal{K}_1) - 1]^2 \right) \left( \mathcal{I}m(\mathcal{K}_2)^2 (\lambda_1 + \lambda_2)^2 + [(\lambda_1 + \lambda_2)\mathcal{R}e(\mathcal{K}_2) - 1]^2 \right)}$$

In order to determine the real and imaginary parts of  $\mathcal{K}_1$  and  $\mathcal{K}_2$ , we can decompose each term appearing in the preceding expressions:

- $a_j = \mathcal{R}e \left( \frac{\sqrt{\frac{i\omega}{D_j(0)}}}{i\omega + \lambda_{n,j}^2} \right) = \sqrt{\frac{\omega}{2D_j(0)}} \left( \frac{\lambda_{n,j}^2 + \omega}{\omega^2 + \lambda_{n,j}^4} \right)$
- $b_j = \mathcal{I}m \left( \frac{\sqrt{\frac{i\omega}{D_j(0)}}}{i\omega + \lambda_{n,j}^2} \right) = \sqrt{\frac{\omega}{2D_j(0)}} \left( \frac{\lambda_{n,j}^2 - \omega}{\omega^2 + \lambda_{n,j}^4} \right)$
- $c_1 = \mathcal{R}e \left( \exp \left( \sqrt{\frac{i\omega}{D_1(0)}} x \right) \right) = \cos \left( \sqrt{\frac{\omega}{2D_1(0)}} x \right) \exp \left( \sqrt{\frac{\omega}{2D_1(0)}} x \right)$
- $d_1 = \mathcal{I}m \left( \exp \left( \sqrt{\frac{i\omega}{D_1(0)}} x \right) \right) = \sin \left( \sqrt{\frac{\omega}{2D_1(0)}} x \right) \exp \left( \sqrt{\frac{\omega}{2D_1(0)}} x \right)$
- $c_2 = \mathcal{R}e \left( \exp \left( -\sqrt{\frac{i\omega}{D_2(0)}} x \right) \right) = \cos \left( \sqrt{\frac{\omega}{2D_2(0)}} x \right) \exp \left( -\sqrt{\frac{\omega}{2D_2(0)}} x \right)$
- $d_2 = \mathcal{I}m \left( \exp \left( -\sqrt{\frac{i\omega}{D_2(0)}} x \right) \right) = -\sin \left( \sqrt{\frac{\omega}{2D_2(0)}} x \right) \exp \left( -\sqrt{\frac{\omega}{2D_2(0)}} x \right)$
- $e_j = \mathcal{R}e \left( \frac{1}{\lambda_j + \sqrt{i\omega D_j(0)}} \right) = \frac{\lambda_j + \sqrt{\frac{D_j(0)\omega}{2}}}{\lambda_j^2 + D_j(0)\omega + \lambda_j \sqrt{2D_j(0)\omega}}$
- $f_j = \mathcal{I}m \left( \frac{1}{\lambda_j + \sqrt{i\omega D_j(0)}} \right) = -\frac{\sqrt{\frac{D_j(0)\omega}{2}}}{\lambda_j^2 + D_j(0)\omega + \lambda_j \sqrt{2D_j(0)\omega}}$

Thanks to these equalities we can recast  $\mathcal{K}_j$  in the following form:

$$\begin{aligned}\mathcal{K}_1 &= (e_1 + if_1) \left( 1 - \sum_n (a_1 + ib_1) \Phi_{n,1}(0) \int_{-L_1}^0 \tilde{D}_1(x) \frac{d\Phi_{n,1}}{dx} (c_1(x) + id_1(x)) dx \right) \\ \mathcal{K}_2 &= (e_2 + if_2) \left( 1 + \sum_n (a_2 + ib_2) \Phi_{n,2}(0) \int_0^{L_2} \tilde{D}_2(x) \frac{d\Phi_{n,2}}{dx} (c_2(x) + id_2(x)) dx \right)\end{aligned}$$

and by noting

$$\begin{aligned}g_1 &= \sum_n \left[ a_1 \int_{-L_1}^0 \tilde{D}_1(x) \frac{d\Phi_{n,1}}{dx} c_1(x) dx - b_1 \int_{-L_1}^0 \tilde{D}_1(x) \frac{d\Phi_{n,1}}{dx} d_1(x) dx \right] \Phi_{n,1}(0) \\ h_1 &= \sum_n \left[ b_1 \int_{-L_1}^0 \tilde{D}_1(x) \frac{d\Phi_{n,1}}{dx} c_1(x) dx + a_1 \int_{-L_1}^0 \tilde{D}_1(x) \frac{d\Phi_{n,1}}{dx} d_1(x) dx \right] \Phi_{n,1}(0) \\ g_2 &= \sum_n \left[ a_2 \int_0^{L_2} \tilde{D}_2(x) \frac{d\Phi_{n,2}}{dx} c_2(x) dx - b_2 \int_0^{L_2} \tilde{D}_2(x) \frac{d\Phi_{n,2}}{dx} d_2(x) dx \right] \Phi_{n,2}(0) \\ h_2 &= \sum_n \left[ b_2 \int_0^{L_2} \tilde{D}_2(x) \frac{d\Phi_{n,2}}{dx} c_2(x) dx + a_2 \int_0^{L_2} \tilde{D}_2(x) \frac{d\Phi_{n,2}}{dx} d_2(x) dx \right] \Phi_{n,2}(0)\end{aligned}$$

we obtain

$$\begin{aligned}\mathcal{K}_1 &= (e_1(1 - g_1) + f_1 h_1) + i(f_1(1 - g_1) - e_1 h_1) \\ \mathcal{K}_2 &= (e_2(1 + g_2) - f_2 h_2) + i(f_2(1 + g_2) + e_2 h_2)\end{aligned}$$

Hence the convergence factor  $\rho$  thanks to (A.2).